

A molecular weight dependent fracture transition in polymethylmethacrylate

W. DÖLL

Institut für Festkörpermechanik, Fraunhofer-Gesellschaft e.V., D-78 Freiburg i.Br., Germany

A novel method which uses an electro-optical arrangement to measure crack velocities in transparent materials is described. It is applied to fast cracks in polymethylmethacrylate of different molecular weights; in polymethylmethacrylate of weight average molecular weight $M_w = 163\,000$ there is a transition in the appearance of the fracture surface, which changes from smooth to coarse-structured rib-like roughness, associated with a transition in the measured crack velocity. This effect and possible causes are discussed.

1. Introduction

Fracture surfaces of polymethylmethacrylate (PMMA) have been described and investigated by various authors [1-8] over the past quarter-century. Amongst the salient features of these investigations – which were mostly performed on commercial grades of PMMA (molecular weights in the range of some millions) – were the parabolic markings [1, 2] and the colours of the fracture surfaces. The origin of the colours was attributed to thin-layer interference of incident white light [3, 4]. The thin layer consists of oriented material of lower refractive index and density [5] than the bulk and results from the process of crazing which accompanies crack propagation in many glassy thermoplastics. Changes in the appearance of fracture surfaces with molecular weight have been reported [6]; in particular the fracture surfaces of PMMA with molecular weights less than 490 000 show well-defined ribs, which were interpreted as hesitation lines [6].

Although these effects arise at high crack propagation rates (of the order of 100 m sec^{-1}) the crack velocities were only measured in relatively few cases [2, 7, 8]. In general, it was found that the appearance of the fracture surfaces could be qualitatively related to the crack velocity.

In this work a novel method for crack velocity measurement is described. This method has already been applied to investigations of the effect of molecular weight on the fracture process in PMMA [9], and in the present work some further results of these investigations are

reported. In particular, an effect is described in which a transition in the appearance of the fracture surface together with a transition in the crack velocity is associated with a specific molecular weight.

2. Experiments

2.1. Materials and testing

The experiments were performed on PMMA of nine different weight average molecular weights, M_w , in the range $110\,000 \leq M_w \leq 8\,000\,000$. Single-edge-notched plate specimens measuring $200 \times 40 \times 4\text{ mm}^3$, were prepared containing sharp notches made by splitting with a wedge. The specimens were tested in a 50 MN Zwick tensile machine at room temperature and with a constant cross-head separation rate of 12 mm min^{-1} ; the load-time curve was recorded and the crack velocity during fast crack propagation was measured.

2.2. Crack velocity measurement

The crack velocity in the fast fracture region was measured with the aid of an electro-optical method developed by the author [10]. This method can be applied to transparent materials and works in the following way.

Owing to the high stress concentrations at the crack tip, there occur local changes in thickness and in refractive index of the material. In a schlierenoptical arrangement [11] as depicted in Fig. 1, parallel light from the light source, L, passes normally through the specimen, S, and is then brought to focus on the knife edge, K. Only that light which is deflected by the refrac-

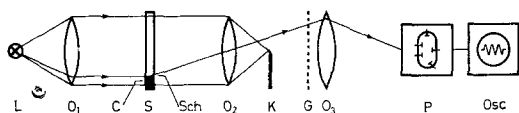


Figure 1 Schlierenoptical arrangement (showing light paths) for crack velocity measurements. L = light source, O = objectives, S = specimen, C = crack, Sch = refracting flaw, K = knife-edge, G = grid, P = photomultiplier, Osc = oscilloscope.

ting flaw, Sch, around the crack tip is not screened by the knife edge, K, and forms a small light spot in the image plane of the objective, O_2 . A grid, G, placed in this image plane is alternately transparent and opaque to light in the direction of crack propagation. Light transmitted by the grid is focused by the objective O_3 onto the cathode of a fast photomultiplier (risetime $0.1 \mu\text{sec}$), whose electrical signal is displayed by the oscilloscope, Osc.

During the fracture of a specimen, the light spot in the image plane follows the crack tip across the specimen at the crack speed. It thus passes over the transparent and opaque strips of

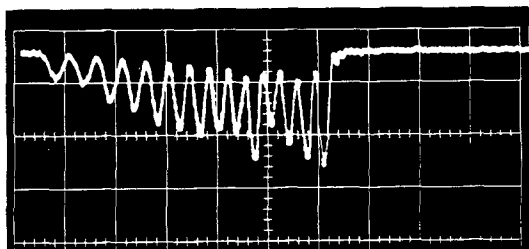


Figure 2 Oscillogram of a fast fracture in PMMA of $M_w = 8\,000\,000$ (large horizontal unit = $20 \mu\text{sec}$).

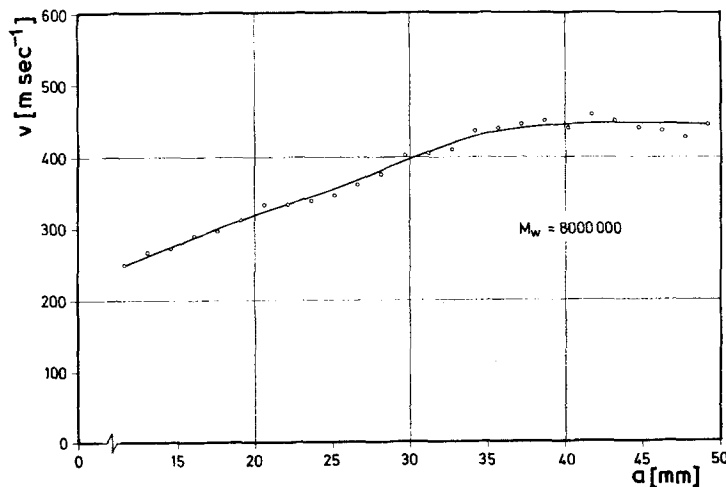


Figure 3 Crack speed v versus crack length a in PMMA of $M_w = 8\,000\,000$ (evaluation of Fig. 2).

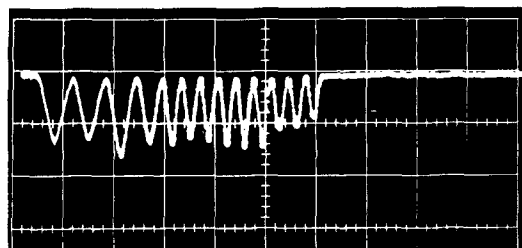


Figure 4 Oscillogram of a fast fracture in PMMA of $M_w = 163\,000$ (large horizontal unit = $20 \mu\text{sec}$).

the grid and onto the photomultiplier; these changes in light intensity generate an alternating signal on the oscilloscope.

Figs. 2 and 4 show two oscillograms of fast fractures in PMMA. By measuring the time between successive maxima or minima of intensity and knowing the grid spacing and the magnification of the optical system the crack speed can be determined. Figs. 3 and 5 show the crack speed versus crack length curves evaluated from Figs. 2 and 4. In these experiments the width of the grid strips was 1.5 mm .

It should be noted that the width of the light spot was nearly as wide as one strip of the grid and that the maximum intensity of the light spot lagged behind the crack tip by approximately 0.2 mm . The accuracy with which a crack velocity curve can be determined is estimated to be better than 5% .

This method of measurement is distinguished by the relative straightforwardness with which the results can be evaluated, and by the large amount of data which can be obtained from a single specimen.

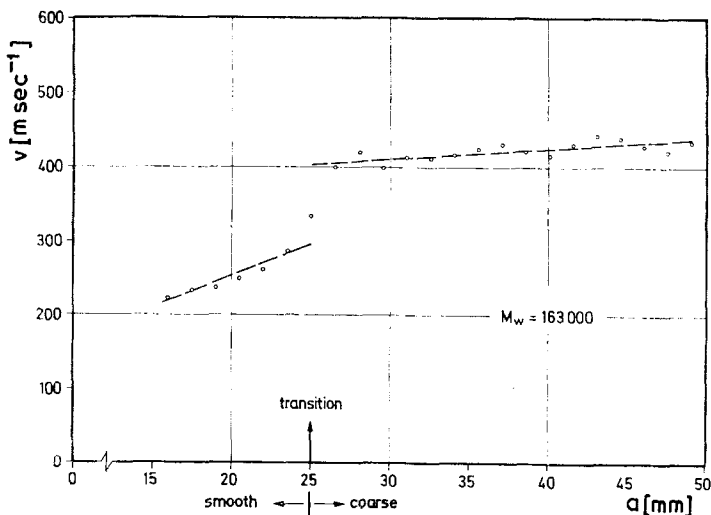


Figure 5 Crack speed v versus crack length a in PMMA of $M_w = 163\,000$ (evaluation of Fig. 4).

3. Experimental results and discussion

3.1. Appearance of the fracture surfaces

The fracture surfaces of PMMA with molecular weights $M_w \geq 490\,000$ show the well-known parabolic markings in the crack speed range 200 to 500 m sec⁻¹, whose number increases with crack speed until roughness occurs (crack speeds $> \sim 500$ m sec⁻¹). In the region of severe roughness (600 to 700 m sec⁻¹) only very few parabolas could be found.

In contrast to this, the fracture surfaces of PMMA with $M_w = 110\,000$ and 120 000 show coarse-structured features immediately at the onset of fast crack propagation (~ 200 m sec⁻¹) which are rib-like in appearance. At higher crack speeds (~ 500 m sec⁻¹) the roughness becomes more like that observed in the higher molecular weight materials but with the rib-like features superimposed. It should be noted that in

these materials no parabolic markings could be found.

The fracture surfaces of PMMA with $M_w = 163\,000$ partially combine the characteristics of both the higher and the lower molecular weight materials, but there is a distinct transition between the two regions. Fig. 6 shows an example of such a fracture surface. The crack propagation direction is from left to right. At the beginning the fracture is almost smooth and shows only parabolic markings as in the higher molecular weight materials. There is then a sharp change to a region of coarse-structured roughness which is similar to that observed in the lower molecular weight materials, but with the rib-like features more pronounced and regular. Another difference is that in this material there are parabolic markings between these rib-like features.

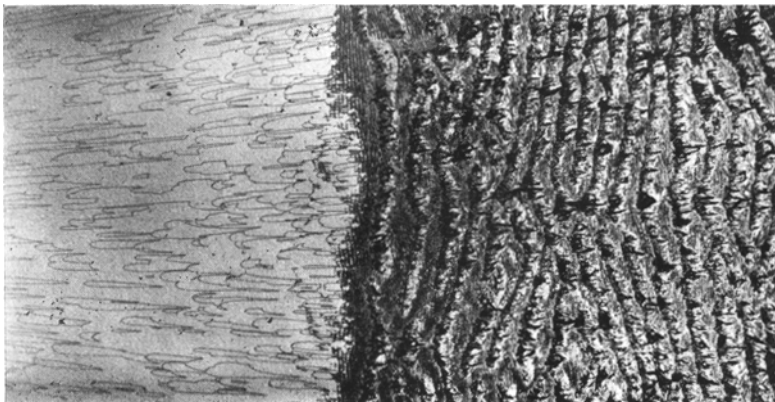


Figure 6 General view of the transition from smooth to coarse in the fracture surface of PMMA of $M_w = 163\,000$. Specimen thickness shown corresponds to 3.6 mm. (Crack propagation direction from left to right.)

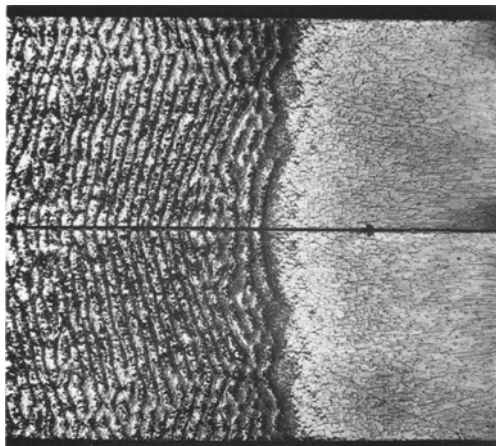


Figure 7 General view of both fracture surfaces, showing the smooth-coarse transition in PMMA of $M_w = 163\,000$. Thickness of the specimen 3.75 mm. (Crack propagation direction from right to left.)

3.2. Crack speed transition behaviour

Associated with the transition from smooth to rough in the fracture surface of PMMA with $M_w = 163\,000$, there is a very sharp increase in the crack speed which is not found in PMMA of other molecular weights. To illustrate this effect the crack speed behaviour in PMMA with $M_w = 8\,000\,000$ and $M_w = 163\,000$ recorded

by the electro-optical method with an equispaced grid of 1.5 mm is shown in Figs. 2 and 4, respectively, and the development of the crack speed can be compared in Figs. 3 and 5. Fig. 3 shows that for PMMA of $M_w = 8\,000\,000$, the rate of increase of crack speed is practically constant in the range 200 to 400 m sec⁻¹; the corresponding fracture surface shows an increasing number of parabolic markings in this region. For PMMA of $M_w = 163\,000$ the increase of crack speed with crack length is shown in Fig. 5. The abrupt increase in the crack speed occurs at that crack length at which the transition from smooth to rough fracture surface takes place. The resolving power of the electro-optical method of measurement is not sufficient to discriminate between a discontinuous jump in crack speed and a continuous, albeit steep, increase at the crack length corresponding to the fracture surface transition. It is, however, possible to characterize the crack speed transition by a notional jump obtained by extrapolation of the crack speed versus crack length plots to the transition point (Fig. 5). From measurements on twelve specimens it was estimated that the maximum speed in the smooth region was $v = 298 \pm 17$ m sec⁻¹ and the minimum speed in the rough region was $v = 406 \pm 11$ m sec⁻¹. Thus the magnitude of the notional jump amounted to 108 ± 16 m sec⁻¹. It may be

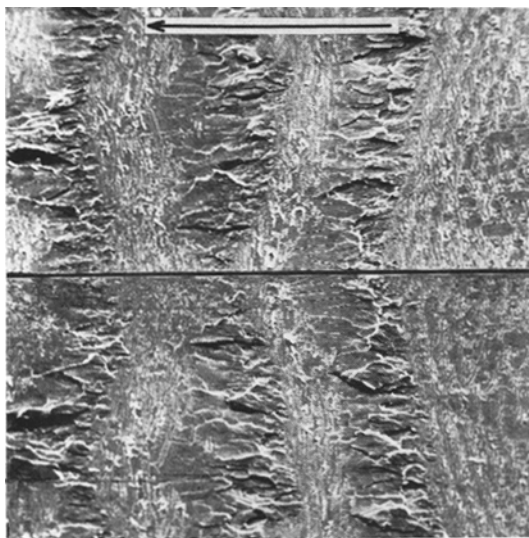


Figure 8

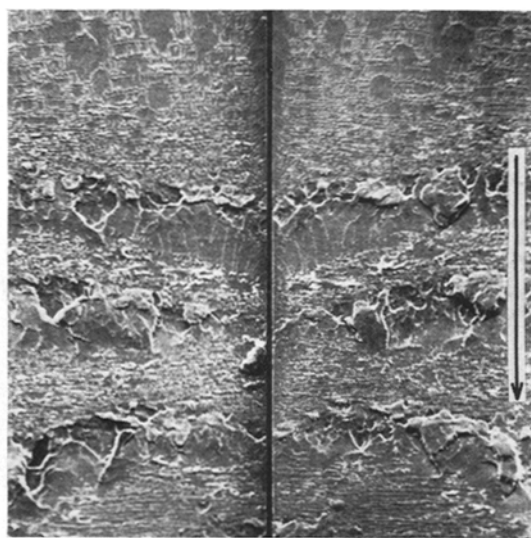


Figure 9

Figures 8 and 9 Rib-like feature on both fracture surfaces as seen from two different directions (cf. Fig. 7), $\times 70$. (Crack propagation direction indicated by arrows.)

noticed that in Fig. 5 the measured point at $v = 333 \text{ m sec}^{-1}$ shown at the transition is a result of the averaging inherent to the method. This value is in good agreement with the mean crack speed of 341 m sec^{-1} calculated from the maximum and minimum speeds given above.

3.3. Strain energy release rate at the transition

Knowing the crack length at the transition, a_t , and the fracture stress, σ , the strain energy release rate, G_t , at the transition can be determined. For edge cracks which are very short compared with the width of the specimen, and for plane strain conditions G is given by

$$G = 1.27\pi \frac{\sigma^2 a}{E} (1 - \nu^2) \quad (1)$$

where E is Young's modulus and ν is Poisson's ratio [12]. From 23 experiments on PMMA of $M_w = 163\,000$, in which the crack lengths at the transition lay in the range $0.07 \leq a_t/W \leq 0.45$ ($W =$ plate width), a mean value and standard deviation of the strain energy release rate of $G_t = 0.83 \pm 0.10 \text{ kJ m}^{-2}$ was determined, using a dynamic value of $E = 4.84 \text{ GN m}^{-2}$ and $\nu = 0.36$.

In the static case, it is usual to apply a finite width correction factor [13] to Equation 1 when a_t/W becomes greater than about 0.05. Applying this correction to the above results gives a strain energy release rate $G_t = 1.43 \pm 0.79 \text{ kJ m}^{-2}$, which has the very high coefficient of variation of 55%.

Similarly, for other phenomena associated with rapid crack propagation which occur at specific crack speeds, such as crack branching [14], it is generally found that the values of strain energy release rate calculated from Equation 1 show very much smaller coefficients of variation than they do when the finite width correction is applied. A possible physical basis for this is that as the crack speed becomes a significant fraction of the sound wave velocity in the material, the presence of the boundaries of the specimen no longer has time to influence the crack tip stress field, and thus the crack behaves as if the boundaries remained remote.

It should be noted that using a dynamic solution for G , for example the crack speed dependent correction function of Broberg [15], the values of the strain energy release rate calculated both with and without the finite width

correction are reduced by the same constant factor.

3.4. Investigation of the rib-like features

A question that arises concerning the transition in the fracture surface appearance and the associated change in crack speed in PMMA of $M_w = 163\,000$ is whether this indicates a change in the fracture process from brittle fracture in the smooth region to ductile fracture in the rough region.

In order to clarify this question, the fracture surfaces were examined by both optical and scanning electron microscopy. Fig. 7 shows an optical micrograph of both fracture surfaces side by side. It is striking that the rib-like features not only form a regular looking pattern on each fracture surface but also that the fracture surfaces appear to be mirror images of each other, as opposed to prominences on one corresponding to depressions on the other. If it is true that raised features on one surface are matched with raised features on the other (and similarly with sunken features) then this would imply that some sort of ductile tearing process was involved in the fracture. However, an examination of the fracture surfaces in more detail using a scanning electron microscope provides rather different information.

Figs. 8 and 9 show scanning electron micrographs of the first three rib-like features of Fig. 7, viewed in two different directions. It can be seen from both figures that the rib-like features are made up of an irregular series of large area prominences and depressions and that the prominences on one fracture surface match with the depressions on the other. This becomes particularly clear at higher magnifications as can be seen in the micrographs of the second rib-like feature of Figs. 8 and 9 shown in Figs. 10a, b and 11a, b for the two different viewing directions. Not only are the coarser structures on each fracture surface complementary, but also the finer, thinner features on both surfaces appear to complement each other. This implies that the material had failed in an essentially brittle manner.

3.5. Discussion

Lines or rib-like features, which occur in an approximately regular manner on fracture surfaces of high polymers accompanying fast fracture, have been reported by different authors for materials such as epoxy resin [16],

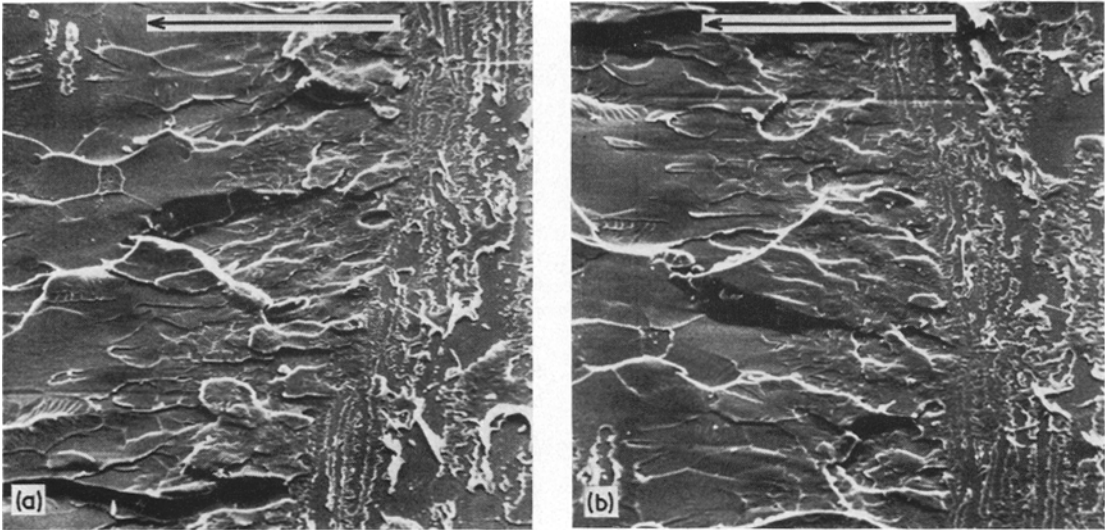


Figure 10 (a) and (b) Second rib-like feature of Fig. 8 at higher magnification ($\times 350$). (Crack propagation direction indicated by arrows.)

carbon-filled rubber [17], polymethylmethacrylate [6], polycarbonate [18] and polystyrene [19]. The nature of these features appears as a more or less regular series of rough ribs separated by smoother regions on the fracture surface. There are differences in the regularity of the features, which can be non-intersecting and almost periodic as in polycarbonate [18], or

intersecting and with a less well-defined regularity as in PMMA. Moreover, there are differences in the spacings of the lines which, depending on the material, can range from a few microns up to several hundred microns. In PMMA, for example, the measured average line spacings in this work are approximately $220 \mu\text{m}$ for $M_w = 163\,000$ and approximately $90 \mu\text{m}$ for

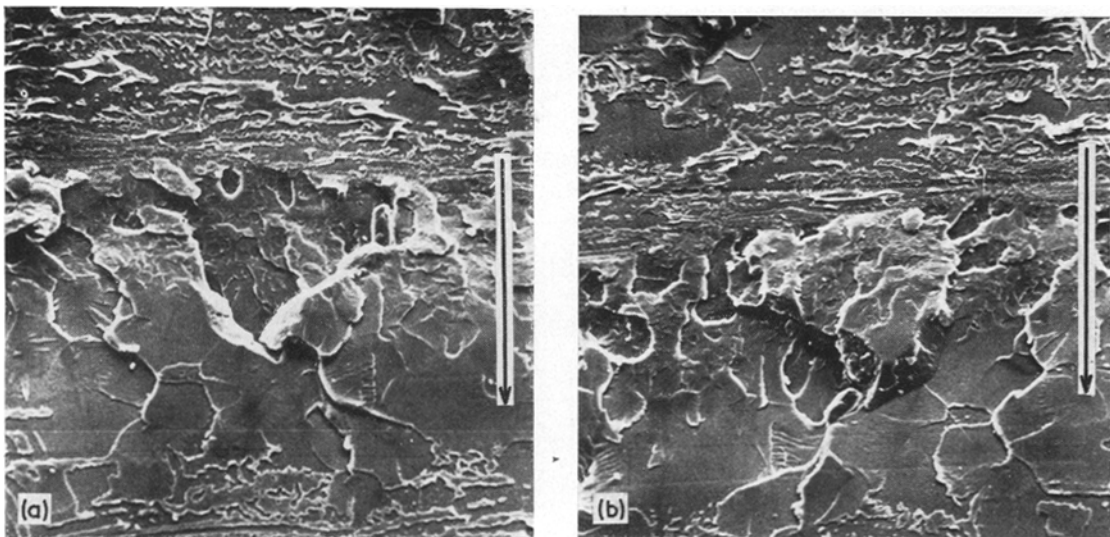


Figure 11 (a) and (b) Second rib-like feature of Fig. 9 at higher magnification ($\times 350$). (Crack propagation direction indicated by arrow.)

$M_w = 110\,000$. From the crack speeds it can be estimated that the frequencies associated with these lines lie in the MHz range.

As a mechanism for the formation of the lines in carbon-filled rubber, PMMA and polycarbonate, various authors [6, 17, 18] have suggested a kind of Wallner effect. Wallner lines are produced by the interaction of the crack front with a transverse wave, through which the direction of the normal stress acting at the crack tip and thus the direction of crack propagation are momentarily deflected. The formation of such lines was first described by Wallner for glass, where they usually appear as very faint lines whose spacing shows almost no regularity since the transverse waves arise from interactions between the stress field of the crack and inhomogeneities which tend to be randomly dispersed. If the regular features found on fracture surfaces of high polymers are to be interpreted in terms of Wallner lines, then this would require a source of regularly generated transverse waves. The origin of such a source is not considered in any detail by the authors cited above. A further difficulty with such an interpretation is that, in particular for PMMA, the stress amplitudes of the transverse waves would have to be very large in order to produce deflections of the crack front as great as found in Figs. 10 and 11. Such high stress amplitudes seem unlikely to occur in PMMA since the damping is large in the frequency range of the postulated transverse waves. Ultrasonic ripple markings, which are artificially produced Wallner lines, are very faint in PMMA [2]. Further it should be noted that there is an additional difference between the Wallner lines in glass and the lines discussed here: the latter show an irregular roughness along the length of the line which are not seen in Wallner lines.

An alternative interpretation of the lines found on the fracture surfaces of PMMA and polystyrene is given by Wolock and Newman [6] and Hull [19] who consider them to be hesitation lines generated by stepwise crack propagation. An experimental verification of this postulated mode of crack propagation would require a method of observing the crack tip region at high magnification whilst following the running crack at the high speeds involved, and would present considerable difficulties.

As a mechanism for the formation of regular ribbed markings on the fracture surface of polystyrene, which they called mackerel pattern,

Murray and Hull [20] suggested that the crack propagates along the interface between the craze and the bulk material and jumps from one interface to the other. The banded structure then arises from the alternating thicknesses of crazed material left on the fracture surface.

Their assumption that the distances between the lines are dependent on craze length and stress can be supported by the observations here. The lines in PMMA of $M_w = 163\,000$ have a larger spacing and are formed at a higher value of strain energy release rate than those in PMMA of $M_w = 110\,000$ or $120\,000$. Craze zone lengths, which can be estimated from the Dugdale model of the plastic zone at a crack tip [21], are also greater in PMMA of $M_w = 163\,000$.

Such differences in strain energy release rate and length of craze zone are not, however, sufficient to explain why no regular line markings are found on the fracture surfaces of high molecular weight PMMA ($M_w \geq 490\,000$). The observations of this work indicate that the occurrence of these lines is dependent on molecular weight. It seems reasonable to infer that this is a reflection of a molecular chain length dependence and that there is a limiting length above which no line markings will be formed.

Acknowledgements

The assistance of Messrs Röhm GmbH, Darmstadt, in providing the materials used in this work is gratefully acknowledged. The author would also like to thank Dr G. W. Weidmann for helpful discussions.

References

1. J. A. KIES, A. M. SULLIVAN and G. R. IRWIN, *J. Appl. Phys.* **21** (1950) 716.
2. F. KERKHOF, in "Kunststoffe Bd. I", edited by R. Nitsche and K. A. Wolf (Springer, Berlin, Göttingen, Heidelberg, 1962), p. 444.
3. M. HIGUCHI, *Repts. Res. Inst. Appl. Mech. Kyushi Univ.* **6** (1958) 173.
4. J. P. BERRY, *J. Polymer Sci.* **50** (1961) 107.
5. R. P. KAMBOUR, *ibid A-2* **4** (1965) 1713.
6. I. WOLOCK and S. B. NEWMAN, in "Fracture Processes in Polymeric Solids", edited by B. Rosen (J. Wiley, New York, London, Sydney, 1964) p. 235.
7. H. SCHARDIN, *Kunststoffe* **44** (1954) 48.
8. B. COTTERELL, *Appl. Mater. Res.* **4** (1965) 227.
9. W. DÖLL, *Eng. Fracture Mech.* **5** (1973) 259.
10. *Idem*, *Wiss. Bericht 3/67 des Ernst-Mach-Institutes, Freiburg i.Br.* (1967).

11. D. W. HOLDER and R. J. NORTH, "Schlieren-Methods", Notes on Applied Science No. 31 (HMSO, London, 1963).
12. G. R. IRWIN, NRL - Report 5120 (1958).
13. B. GROSS, J. E. SRAWLEY and W. F. BROWN JUN, NASA TN D-2395 (1964).
14. W. DÖLL, Dissertation, Universität Karlsruhe (1974).
15. K. B. BROBERG, *J. Appl. Mech.* **31** (1964) 546.
16. G. MANITZ, Dissertation,, Freiburg i.Br. (1959).
17. E. H. ANDREWS, *J. Appl. Phys.* **30** (1959) 740.
18. G. JACOBY and CH. CRAMER, *Rheol. Acta* **7** (1968) 23.
19. D. HULL, *J. Mater. Sci.* **5** (1970) 357.
20. J. MURRAY and D. HULL, *J. Polymer Sci. A-2* (1970) 583.
21. D. S. DUGDALE, *J. Mech. Phys. Solids* **8** (1960) 100.

Received 26 November and accepted 11 December 1974.